• Basic Research •

Protective effects of a novel drug RC28-E blocking both VEGF and FGF2 on early diabetic rat retina

Qian-Hui Yang[1], Yan Zhang[1], Jing Jiang[2], Mian-Mian Wu[1], Qian Han[1], Qi-Yu Bo[1], Guang-Wei Yu[1], Yu-Sha Ru[1], Xun Liu[1], Min Huang[3], Ling Wang[3], Xiao-Min Zhang[1], Jian-Min Fang[4], Xiao-Rong Li[1]

[1]Tianjin Medical University Eye Hospital, Tianjin Medical University Eye Institute, College of Optometry and Ophthalmology, Tianjin Medical University, Tianjin 300384, China

[2]School of Pharmacy, Binzhou Medical University, Yantai 264003, Shandong Province, China

[3]Remegen, Ltd., Yantai 264006, Shandong Province, China

[4]School of Life Sciences and Technology, Tongji University, Shanghai 200092, China

Co-first authors: Qian-Hui Yang, Yan Zhang, Jing Jiang and Mian-Mian Wu

Correspondence to: Jian-Min Fang. School of Life Sciences and Technology, Tongji University, Shanghai 200092, China. jfang@tongji.edu.cn; Xiao-Rong Li. Tianjin Medical University Eye Hospital, Tianjin Medical University Eye Institute, College of Optometry and Ophthalmology, Tianjin Medical University, Tianjin 300384, China. xli@tmu.edu.cn

Received: 2018-02-02 Accepted: 2018-04-24

Abstract

• AIM: To investigate protective effects of a novel recombinant decoy receptor drug RC28-E on retinal damage in early diabetic rats.

• METHODS: The streptozotocin (STZ)-induced diabetic rats were randomly divided into 6 groups: diabetes mellitus (DM) group (saline, 3 μL/eye); RC28-E at low (0.33 μg/μL, 3 μL), medium (1 μg/μL, 3 μL), and high (3 μg/μL, 3 μL) dose groups; vascular endothelial growth factor (VEGF) Trap group (1 μg/μL, 3 μL); fibroblast growth factor (FGF) Trap group (1 μg/μL, 3 μL). Normal control group was included. At week 1 and 4 following diabetic induction, the rats were intravitreally injected with the corresponding solutions. At week 6 following the induction, apoptosis in retinal vessels was detected by TUNEL staining. Glial fibrillary acidic protein (GFAP) expression was examined by immunofluorescence. Blood-retinal barrier (BRB) breakdown was assessed by Evans blue assay. Ultrastructural changes in choroidal and retinal vessels were analyzed by transmission electron microscopy (TEM). Content of VEGF and FGF proteins in retina was measured by enzyme linked immunosorbent assay (ELISA). The retinal expression of intercellular cell adhesion molecule-1 (ICAM-1), tumor necrosis factor-α (TNF-α), VEGF and FGF genes was examined by quantitative polymerase chain reaction (qPCR).

• RESULTS: TUNEL staining showed that the aberrantly increased apoptotic cells death in diabetic retinal vascular network was significantly reduced by treatments of medium and high dose RC28-E, VEGF Trap, and FGF Trap (all $P<0.05$), the effects of medium and high dose RC28-E or FGF Trap were greater than VEGF Trap ($P<0.01$). GFAP staining suggested that reactive gliosis was substantially inhibited in all RC28-E and VEGF Trap groups, but the inhibition in FGF Trap group was not as prominent. Evans blue assay demonstrated that only high dose RC28-E could significantly reduce vascular leakage in early diabetic retina ($P<0.01$). TEM revealed that the ultrastructures in choroidal and retinal vessels were damaged in early diabetic retina, which was ameliorated to differential extents by each drug. The expression of VEGF and FGF2 proteins was significantly upregulated in early diabetic retina, and normalized by RC28-E at all dosages and by the corresponding Traps. The upregulation of ICAM-1 and TNF-α in diabetic retina was substantially suppressed by RC28-E and positive control drugs.

• CONCLUSION: Dual blockade of VEGF and FGF2 by RC28-E generates remarkable protective effects, including anti-apoptosis, anti-gliosis, anti-leakage, and improving ultrastructures and proinflammatory microenvironment, in early diabetic retina, thereby supporting further development of RC28-E into a novel and effective drug to diabetic retinopathy (DR).

• KEYWORDS: diabetic retinopathy; vascular endothelial growth factor; fibroblast growth factor 2; recombinant decoy receptor; retinal damage; diabetes

DOI:10.18240/ijo.2018.06.07

Citation: Yang QH, Zhang Y, Jiang J, Wu MM, Han Q, Bo QY, Yu GW, Ru YS, Liu X, Huang M, Wang L, Zhang XM, Fang JM, Li XR. Protective effects of a novel drug RC28-E blocking both VEGF and FGF2 on early diabetic rat retina. *Int J Ophthalmol* 2018;11(6):935-944

INTRODUCTION

Diabetes mellitus (DM) threatens the public health with the rising prevalence around the globe. Diabetic retinopathy (DR), one of the servere microvascular complications of DM[1], is the leading cause of blindness in the working age population[2]. Thus far, the majority of therapeutic modalities to DR have focused on symptom relief. For example, laser therapy prevents dramatic deterioration in visual function, yet hardly improves visual acuity and generates damage in neuroretina[3]. Glucocorticoid drugs can alleviate diabetic macular edema caused by breakdown of blood-retinal barrier (BRB) and retinal vessel leakage, however they may cause adverse effects such as cataract, elevated intraocular pressure[4-5] and endophthalmitis. In addition, surgeries like vitrectomy are traumatic, and their efficacies on restoring visual functions are not satisfactory[6]. Therefore, it is necessary to develop a novel, effective, and safe therapeutic modality based on the pathogenesis of DR.

Up to now, vascular endothelial growth factor (VEGF) is considered as an important proinflammatory, proangiogenic, and vascular permeability factor in the pathogenesis and development of DR[7], and its protein levels were elevated in the vitreous fluid of the diabetic patients[8]. Emerging ophthalmic drugs thus target this pathogenic factor. For instance, ranibizumab is an Fab fragment of a humanized monoclonal antibody to VEGF[9], and conbercept is a recombinant decoy receptor that fuses human IgG1 Fc with the Fab fragment containing domain 2 of VEGF receptor 1 (VEGFR1) and domains 3 and 4 of VEGFR2[10]. However, the main problems incurred by the anti-VEGF drugs include more than 50% non-response rate and rapid drug resistance[6,11], indicating that the factors besides VEGF might also be responsible for DR pathogenesis.

Previous studies have suggested that fibroblast growth factor 2 (FGF2) expression is upregulated both in the retinas of diabetic animals[12-14] and in the vitreous samples of diabetic patients[15-16]. At the cellular and molecular level, FGF2 acts as a potent mitogen for vascular endothelial cells[17], and exerts a synergistic effect on biological activities of VEGF[18]. Furthermore, numerous studies have implicated that simultaneous targeting on VEGF and FGF2 may be more efficacious in treating angiogenesis-related diseases[19-20]. Based on this rationale, a novel recombinant decoy receptor drug, designated as RC28-E (Remegen, Ltd., Yantai Biopharm aceutical company, China), that can bind both VEGF and FGF2 with high affinity and specificity. The Fab fragment of RC28-E contains domain 2 of VEGFR1, domain 3 of VEGFR2, as well as domains 2 and 3 of FGFR1[21]. The anti-angiogenic effects of RC28-E have been confirmed both in vascular endothelial cells and in xenograft tumor model[21]. Therefore, it is hypothesized that RC28-E may generate protective effects on early diabetic retina by dual blockade of VEGF and FGF2. To test this hypothesis, RC28-E was intravitreally injected into streptozotocin (STZ)-induced early diabetic rats, 6wk following the diabetic induction, the apoptosis of retinal vessels, the activation of retinal glial cells, the BRB breakdown, the ultrastructural changes in retinal and choroidal vessels, and the expression of proinflammatory factors were examined. In the meanwhile, VEGF Trap, a decoy receptor of VEGF that has already been used in the clinics[22] and FGF Trap, a decoy receptor of FGF2 containing domains 2 and 3 of FGFR1 in its Fab fragment[23], were included as positive control drugs. This study provides experimental bases for further development of RC28-E into a novel drug to DR.

MATERIALS AND METHODS

Animals Male Sprague-Dawley (SD) rats (age 8-10wk, body weight 220-250 g) were purchased from Experimental Animal Center in the Chinese Academy of Military Medical Sciences. Rats were housed in specific pathogen free animal facility of Tianjin Medical University, and fed *ad lib* with food and drink. The ambient temperature was 25℃±1℃, the relative humidity was 40%±5%, and the illumination was under 12-h light: 12-h dark cycle. All animal experiments were approved by the Institutional Animal Care and Use Committee of Tianjin Medical University (permission number: SYXK2009-0001), and in accord with the ARVO Statement for the Use of Animals in Ophthalmic and Vision Research.

Diabetic Induction The rats were injected with 2% STZ dissolved in sodium citrate buffer (pH 4.5; Amresco Chemical Co., Solon, OH, USA) at 45 mg/kg through vena caudalis to induce diabetes. At 72h following the injection, the rats with the blood glucose levels higher than 16.7 mmol/L were considered diabetic and included in the subsequent experiments (n=240); whereas the normal controls (n=40) were intravenously injected with an equal volume of sodium citrate buffer.

Animal Grouping and Intravitreal Injections The diabetic rats were randomly divided into 6 groups (n=40/group): the DM group (saline, 3 μL/eye); VEGF Trap group (VEGF Trap-Eye, Regeneron, Tarrytown, NY, and Bayer HealthCare, Berlin, Germany, 1 μg/μL ×3 μL/eye); FGF Trap group (FGF Trap, Remegen Co., Ltd., Yantai, China, 1 μg/μL ×3 μL/eye); low dose RC28-E group (RC28-E, Remegen Co., Ltd., Yantai, China, 0.33 μg/μL ×3 μL/eye); medium dose RC28-E group (1 μg/μL ×3 μL/eye); and high dose RC28-E group (3 μg/μL× 3 μL/eye). The normal control group (saline, 3 μL/eye) was also included. All the animals were intravitreally injected in the right eye with the corresponding solution with a microsyringe equipped with a 33 Gauge needle as previously described[24-25]. The intravitreal injections were performed at week 1 and 4 following the intravenous injection.

Physiological Parameters of Streptozotocin-induced Diabetic Rats The body weight of all the experimental

animals were recorded on the weekly basis. The blood glucose levels of all the rats were measured at day 3 and week 6 after the intravenous injection of STZ or sodium citrate buffer. At week 4 following the induction of diabetes, the averaged daily water consumption of the diabetic rats and normal counterparts was monitored for 2wk.

Trypsin Digestion of Retina Followed by TUNEL Staining At week 6 after the intravenous injection, the rats were deeply anesthetized, the eyeballs were fixed in 4% paraformaldehyde (PFA) at 4℃ for 72h. The intact retinas were isolated under a dissection microscope and gently shaken overnight in deionized water at room temperature (RT). The retinas were then transferred to 1% Triton-X 100 (Sigma-Aldrich, St. Louis, MO, USA) and shaken for 2h at 37℃, after which they were subjected to a 2-3h digestion at 37℃ with 3% crude trypsin (Amresco Chemical Co., Solon, OH, USA). Subsequently the retina was mounted on the slide with photoreceptor side upwards. It was extensively flushed with drop-wise deionized water from a curved needle mounted on a 1-mL syringe till the parenchyma was substantially exfoliated, revealing a translucent retinal vascular network. The vascular network was air dried and underwent TUNEL staining using an *In Situ* Cell Death Detection Kit (Roche, Branford, CT, USA) according to the manufacturer's protocol. After the staining, slides were mounted, pictures taken, and TUNEL positive signals analyzed as described previously[25].

Immunofluorescence of Glial Fibrillary Acidic Protein Staining The rats were anesthetized and perfused through left ventricle with cold phosphate buffered solution (PBS) and 1% PFA. The eyeballs were fixed in 4% PFA for 1h at RT, washed with PBS, dehydrated in 10% sucrose for 1h and 20% sucrose for 2h, cryo-embedded in OCT. (Sakura Finetek, Torrance, CA, USA), and stored at -80℃. The comparable part of the frozen eyeballs was cryo-sectioned (5 μm in thickness). The sections were incubated with a primary rabbit polyclonal antibody to glial fibrillary acidic protein (GFAP) (1:1000, Abcam, Cambridge, MA, USA) at 4℃ overnight. After extensive washes, the slides were stained next day with an Alexa 594-conjugated secondary antibody (1:2000, Abcam, Cambridge, MA, USA) at RT for 2h. The slides were mounted with 4',6-diamidino-2-phenylindole (DAPI)-containing ProLong Gold Antifade reagent (Life Technologies, Beijing, China) and photographed under a fluorescence microscope (BX51; Olympus Optical Co. Ltd., Tokyo, Japan) as previously described[25-26].

Evans Blue Assay The BRB breakdown was examined by Evans blue assay at week 6 after the diabetic induction as described elsewhere[24]. Briefly, the rats were injected with Evans blue solution (Biotopped Co., Ltd., Beijing, China) through tail vein. At 2h after the injection, blood (1 mL) was collected from inner canthus and centrifuged. The supernatant was diluted (1:100) with methanamide (Amresco Chemical Co., Solon, OH, USA). The absorbance at 620 nm, with the correction at 740 nm was measured by an Infinite 200 PRO Multimode Microplate Reader (Tecan Group Ltd., Männedorf, Switzerland). The concentration of Evans blue in the blood was calculated. Then the rats were thoroughly perfused with warm sodium citrate buffer. The retinas were isolated and dry weight recorded. The Evens blue dye leaked into the retina parenchyma was extracted with methanamide. The portion with low molecular weight was enriched by ultrafiltration. The absorbance of the filtrate at 620 nm with correction at 740 nm was measured as described above. The permeability of Evans blue in retina was calculated according to the following formula: Permeability [μL/(g·h)]=[Evans blue content in retina (μg)/ retina dry weight (g)] / [time-averaged Evans blue concentration in blood (μg/μL) × circulating time (h)].

Transmission Electron Microscopy The eyeballs, with anterior segments removed, were fixed in a pre-cooled 2.5% glutaraldehyde solution (pH 7.4) followed by 1% osmium tetroxide solution. Then the samples were dehydrated in graded ethanol solutions, treated with propylene oxide, embedded in Epon812, and subjected to ultra-thin sections (about 50 nm). The sections were subsequently stained with uranium acetate and lead citrate, and photographed by a Hitachi-7500 transmission electron microscope (Hitachi, Tokyo, Japan).

Enzyme-linked Immunosorbent Assay At week 6 following the intravenous injection, total proteins of the rat retinas were extracted using a Tissue Protein Extraction Kit (CWbiotech, Beijing, China), and the total protein concentration was determined using a BCA Protein Assay Kit (CWbiotech, Beijing, China). The content of VEGF and FGF2 protein in the retina samples was determined by enzyme linked immunosorbent assays (ELISAs) according to the manufacturer's protocols (Rat VEGF Quantikine ELISA Kit, cat. RRVOO; Mouse/Rat FGF basic Quantikine ELISA Kit, cat. MFB00; R&D systems, Minneapolis, MN, USA), the protein concentration (pg/mL) of VEGF and FGF2 was normalized to the total protein concentration (mg/mL).

RNA Extraction, Reverse Transcription and Quantitative Polymerase Chain Reaction At week 6 after the diabetic induction, total RNA from rat retinas was extracted using a TRIzol Plus RNA Purification Kit (Thermo Fisher Scientific, Waltham, MA, USA), the concentration and purity of total RNA were determined with a Nanodrop Spectrophotometer (Thermo Fisher Scientific, Waltham, MA, USA). Of 1 μg total RNA was reverse transcribed into cDNA using a RevertAid First Strand cDNA Synthesis Kit (Thermo Fisher Scientific, Waltham, MA, USA). The quantitative polymerase chain reaction (qPCR) reaction mixture contained 3 μL of cDNA template, forward and reverse primers of target genes (Table 1),

Table 1 qPCR primers

Gene	NCBI accession No.	Primer sequence
ICAM-1	NM_012967.1	F:5'-CGGGAGATGAATGGTACCTACAA-3'
		R:5'-TGCACGTCCCTGGTGATACTC-3'
TNF-α	NM_012675.3	F:5'-ACAAGGCTGCCCCGACTAC-3'
		R:5'-CTCCTGGTATGAAATGGCAAATC-3'
VEGF	NM_031836.3	F:5'-GGGCCTCTGAAACCATGAACT-3'
		R:5'-TGGTGGAGGTACAGCAGTAAAGC-3'
FGF2	M22427.1	F:5'-AAGGATCCCAAGCGGCTCTA-3'
		R:5'-CGGCCGTCTGGATGGA-3'
GAPDH	NM_017008.4	F:5'-ATGTATCCGTTGTGGATCTGACAT-3'
		R:5'- CTCGGCCGCCTGCTT-3'

ICAM-1: Intercellular cell adhesion molecule-1; TNF-α: Tumor necrosis factor-α; VEGF: Vascular endothelial cell growth factor; FGF2: Fibroblast growth factor 2; GAPDH: Glyceraldehyde-3-phosphate dehydrogenase.

Table 2 Comparison of body weight between diabetic rats and normal rats g

Groups	D 0	D 3	W 1	W 2	W 3	W 4	W 5	W 6
DM								
Average	261.40	255.14	247.17	231.20	262.87	280.34	281.15	296.07
SD	13.38	15.95	24.03	34.09	36.31	43.67	41.82	51.32
Normal								
Average	258.57	288.43[a]	329.21[a]	345.50[a]	366.21[a]	394.69[a]	393.77[a]	421.18[a]
SD	12.70	15.77	19.42	21.59	21.90	26.87	30.58	34.35

D: Day; W: Week; DM: Diabetes mellitus. [a]*P*<0.01 *vs* DM.

and 5 μL SYBR Green FastStart 2X Master Mix (Roche, Branford, CT, USA). The qPCR was performed as previously described[24-25]. Glyceraldehyde-3-phosphate dehydrogenase (GAPDH) was used as reference gene. The data were analyzed by $2^{-\Delta\Delta Ct}$ method.

Statistical Analyses The statistical analyses were performed using SPSS 13.0 software (SPSS Inc., San Diego, CA, USA). The normality of quantitative data was confirmed by Shapiro-Wilk test, and the data were expressed as mean±SD. The homogeneity of variance was verified by Levene test. Then the differences in physiological parameters between DM and normal rats were analyzed by Two-way ANOVA followed by Tukey post hoc; other quantitative data were analyzed by one-way ANOVA followed by Tukey post hoc. A *P* value less than 0.05 was considered significant.

RESULTS

Physiological Parameters During the first 2wk after the diabetic induction, the body weight of diabetic rats showed a slight decrease, and then increased slowly till week 4 following the induction, and remained stable thereafter. By contrast, the body weight of normal rats exhibited a close to linear increment, and was significantly higher than that of the diabetic rats at each time point (all *P*<0.01; Table 2). Three days after the intravenous injection, the blood glucose of diabetic rats was 25.97±4.98 mmol/L, being significantly higher than that of the normal controls (*P*<0.01); at week 6 following the injection, it increased to 32.05±2.65 mmol/L.

Table 3 Comparison of blood glucose between diabetic and normal rats mmol/L

Groups	D 3	W 6
DM	25.97±4.98	32.05±2.65
Normal	8.04±0.95[a]	6.60±0.74[a]

D: Day; W: Week; DM: diabetes mellitus. [a]*P*<0.01 *vs* DM.

Whereas the blood glucose levels of the normal controls at the 2 time points were 8.04±0.95 mmol/L and 6.60±0.74 mmol/L, respectively (Table 3). As for water consumption, the averaged volume of drinking water of diabetic rats was 3-4 fold that of the normal control group (all *P*<0.001, DM *vs* normal; Table 4).

The Apoptotic Cell Death in Retinal Vascular Network The retinal vascular networks were outlined by DAPI counterstaining of cell nuclei (Figure 1). No apoptotic cell death was detected in the normal group; whereas the number of apoptotic cells was significantly increased in the retinal vascular network of DM group as compared to the normal controls (*P*<0.01; Figure 1). The number of apoptotic cells in low dose RC28-E group was decreased, but was not significantly different from that in the DM group (*P*=0.110; Figure 1). The numbers of apoptotic cells in medium and high dose RC28-E groups, VEGF Trap, and FGF Trap groups were significantly lower than that in the DM group (*P*<0.01, medium dose RC28-E *vs* DM; *P*<0.001, high dose RC28-E *vs* DM; *P*<0.01, VEGF Trap *vs* DM; *P*<0.05, FGF Trap *vs* DM; Figure 1). The numbers of apoptotic cells in the medium and high doses RC28-E groups and FGF Trap

Table 4 Comparison of drinking water between diabetic rats and normal rats mL

Groups	D 1	D 2	D 3	D 4	D 5	D 6	D 7	D 8	D 9	D 10	D 11	D 12
DM												
Average	938.75	865.00	885.00	627.50	730.00	792.50	785.00	882.50	990.00	781.25	866.25	808.75
SD	121.35	80.53	93.04	82.07	91.50	114.98	102.26	162.11	84.85	136.85	156.75	196.72
Normal												
Average	206.67[b]	193.33[b]	233.33[b]	180.00[b]	200.00[b]	193.33[b]	166.67[b]	233.33[b]	233.33[b]	140.00[b]	186.67[b]	206.67[b]
SD	61.10	46.19	23.09	20.00	34.64	46.19	46.19	23.09	23.09	0.00	23.09	61.10

D:Day; DM: Diabetes mellitus. [b]P<0.001 *vs* DM.

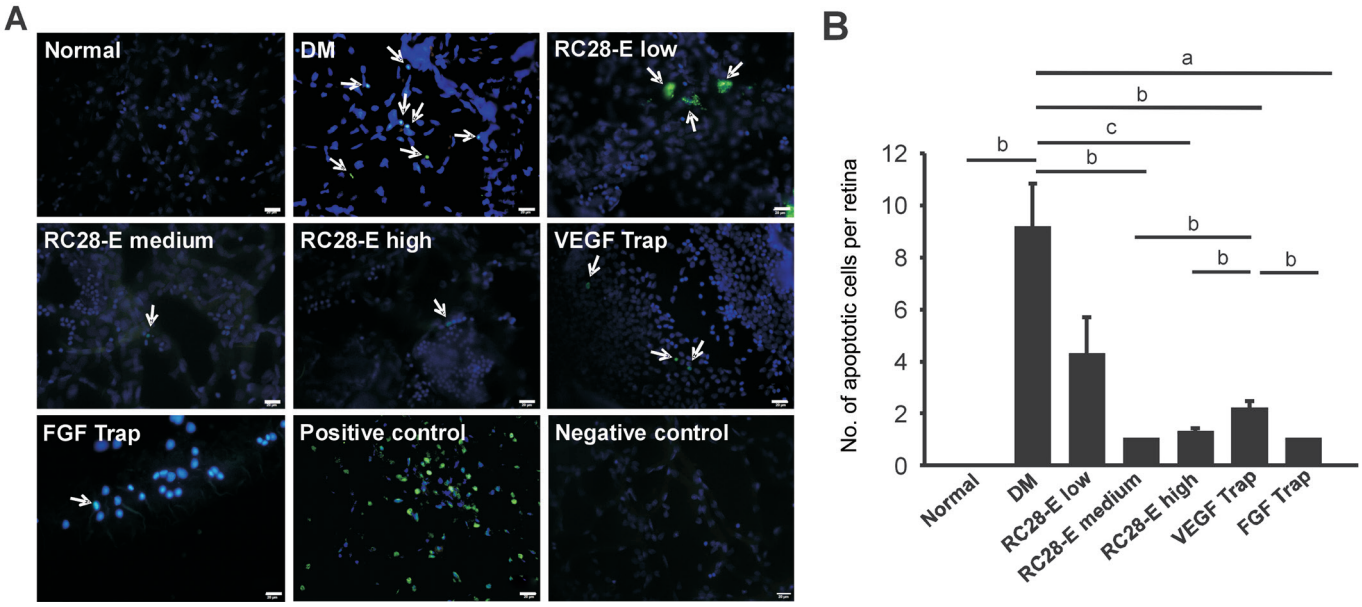

Figure 1 The apoptotic cells death in retinal vascular network of each experimental group A: The representative images of TUNEL staining of retinal vascular network in each group and the positive and negative controls of TUNEL staining. Arrows indicate the TUNEL-positive cells. Scale bar=20 μm. B: The apoptotic cells in each experimental group were quantified. [a]P<0.05, [b]P<0.01, [c]P<0.001.

group were significantly lower than that of VEGF Trap group (P<0.01, medium dose RC28-E *vs* VEGF Trap; P<0.01, high dose RC28-E *vs* VEGF Trap; P<0.05, FGF Trap *vs* VEGF Trap; Figure 1). The results suggest that all the drugs, including RC28-E, VEGF Trap and FGF Trap have an anti-apoptotic effect in early diabetic retinas, and the medium and high dose RC28-E as well as FGF Trap exert better protection from neurodegeneration than low dose RC28-E and VEGF Trap.

Expression and Distribution of Retinal Glial Cell Marker Glial Fibrillary Acidic Protein In the normal retinas, GFAP was mainly localized to the outer nuclear layer (ONL), with scattered filaments and spot-like staining extending into the outer plexiform layer (Figure 2). In contrast, the GFAP staining in the retinas of DM group was predominantly located to the inner nuclear layer, inner plexiform layer, and ganglion cell layer (GCL), and the staining intensity was substantially augmented; moreover, such staining revealed the morphological changes of retinal glial cells, with pseudopodia extending from GCL to ONL, indicating the reactive gliosis in early diabetic retinas (Figure 2). In all the RC28-E treatment groups and VEGF Trap group, only a little GFAP staining was observed in the GCL. In the FGF Trap-treated retinas, GFAP staining was observed across the retinal layers, but with much less intensity than that in the retinas of DM group (Figure 2). These results suggest that RC28-E at all dosages and VEGF Trap may have a greater inhibitory effect on reactive gliosis than FGF Trap in early diabetic retinas.

Blood-retinal Barrier Breakdown and Retinal Vessel Leakage The retinal vascular leakage, as detected by the amount of Evans blue dye in retinal parenchyma, in the DM group was significantly higher than that of the normal control group (P<0.001; Figure 3). Furthermore, treatment of the early diabetic retinas with high dose RC28-E significantly reduced the vascular leakage to the normal level (P<0.001, DM *vs* high dose RC28-E; P=0.137, high dose RC28-E *vs* normal; Figure 3). However, there was no significant difference in the retinal vascular leakage between medium dose RC28-E, low dose EC28-E, VEGF Trap, and FGF Trap groups and DM group (all P>0.05; Figure 3).

Ultrastructural Changes in Retinal Microvessels In the normal group, the basement membranes of choroidal and retinal capillaries were intact, the lumens unobstructed; the

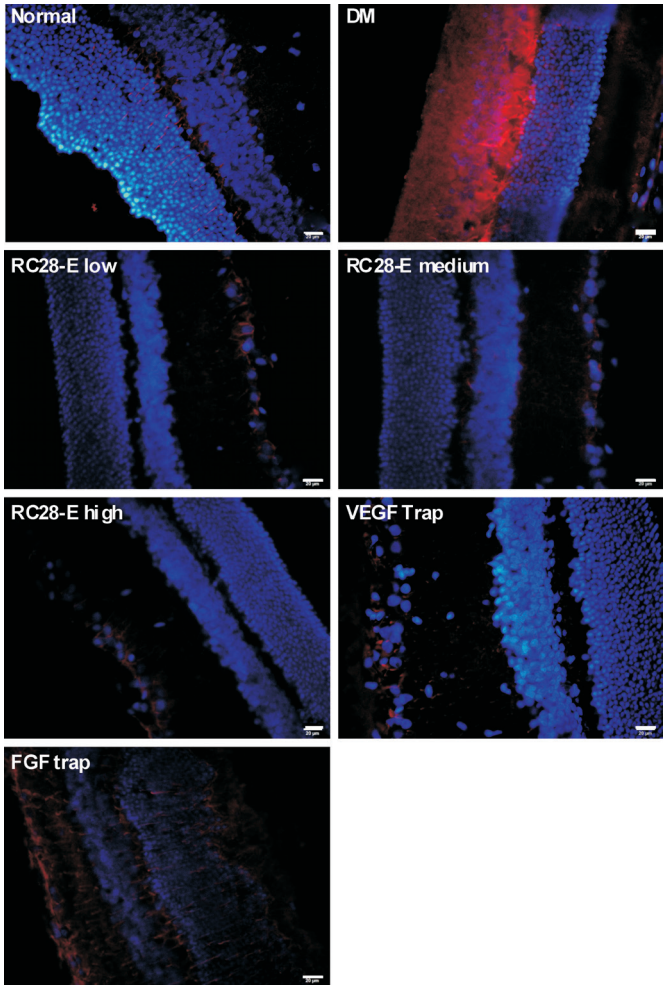

Figure 2 GFAP staining in each experimental group Red fluorescence referred to GFAP positive signal. Blue fluorescence represented DAPI counterstaining, and revealed the structure of retinal layers. Scale bar=20 μm.

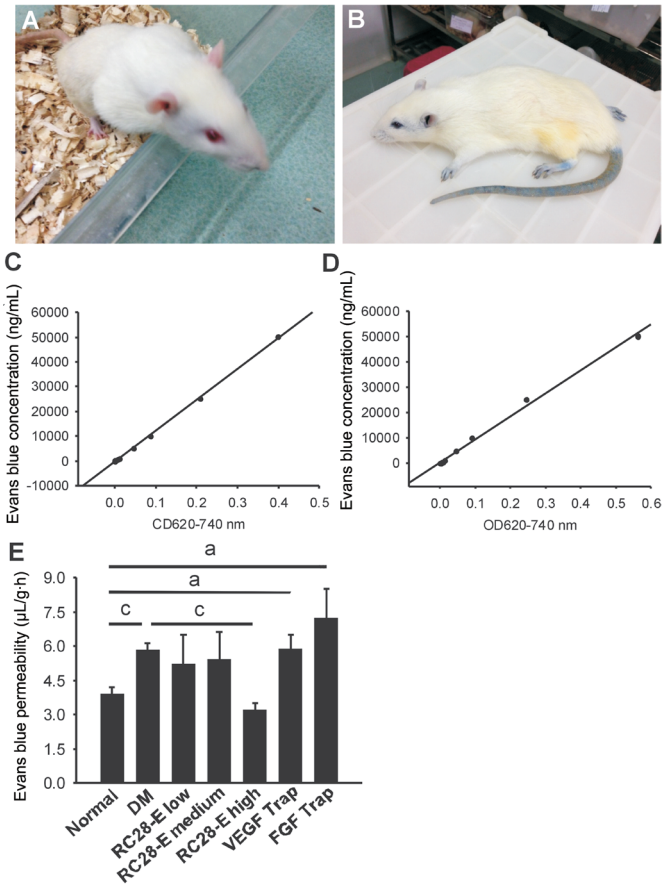

Figure 3 BRB breakdown and vascular leakage in each experimental groups The rats before and after the intravenous injection of Evans blue dye were shown in A and B, respectively. The concentrations of Evans blue dye in the blood and retina were calculated according to the corresponding standard curves C and D. The retinal vessel leakage of Evans blue dye was quantified and shown in E. $^{a}P<0.05$, $^{c}P<0.001$.

nuclei and collagen fibers in the ONL were neatly arranged (Figure 4). While in the DM group, the stratified basement membranes were observed in choroidal and retinal capillaries. The endothelial cells were swelled and protruded towards the lumen, the blood cells were congested, both of which lead to the stenosis and deformation of capillary lumens (Figure 4). Among the RC28-E treatment groups, the most obvious changes lied in the capillary ultrastructures. As the dosage increased, the lumens of choroidal and retinal microvessels became gradually smooth and the basement membrane stratification progressively improved, with the RC28-E at high dose generating the optimal protective effects (Figure 4). In the FGF Trap group, the basement membranes of choroidal microvessels were stratified; the endothelial cells in the retinal vessels approximating the inner limiting membrane protruded toward the lumen, hereby a few vascular lumens were almost occluded (Figure 4). The choroidal capillary basement membranes in the VEGF Trap group were stratified, yet the lumens of both choroidal and retinal vessels were still open (Figure 4).

Expression of Vascular Endothelial Growth Factor and Fibroblast Growth Factor 2 Proteins in the Retinas The expression of VEGF protein in the retina homogenate of DM group was significantly upregulated as compared with that of normal group ($P<0.01$, normal *vs* DM; Figure 5A), however, this upregulation was significantly reduced to the normal level by the intervention of RC28-E at all dosages ($P<0.05$, RC28-E low dose *vs* DM; $P=0.179$, RC28-E low dose *vs* normal; $P<0.01$, RC28-E medium dose *vs* DM; $P=0.435$, RC28-E medium dose *vs* normal; $P<0.05$, RC28-E high dose *vs* DM; $P=0.489$, RC28-E high dose *vs* normal; Figure 5A). As expected, VEGF Trap, but not FGF Trap, significantly reduced the VEGF protein content in the diabetic retina homogenate ($P<0.05$, VEGF Trap *vs* DM; $P=0.156$, FGF Trap *vs* DM; Figure 5A). On the other hand, the FGF2 protein level in the early diabetic retinas was increased as compared to that in the normal controls, and the difference was at the verge of statistical significance ($P=0.060$, normal *vs* DM; Figure 5B). Additionally, low and medium dose RC28-E significantly reduced the FGF2 protein levels (both $P<0.05$; Figure 5B),

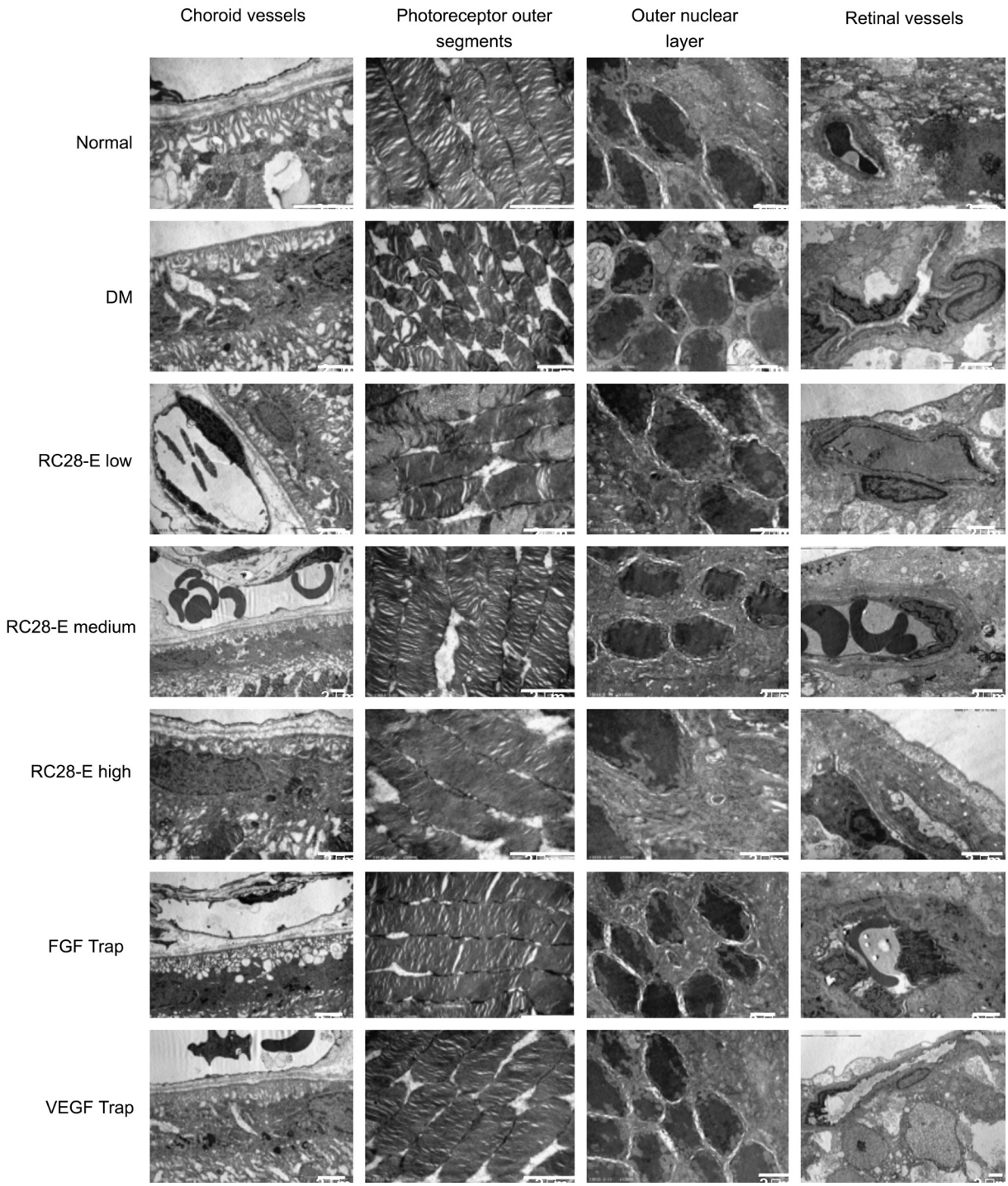

Figure 4 Ultrastructural changes in choroidal and retinal vessels and in neuroretinas The ultrastructural changes in the choroidal vessels, photoreceptor outer segments, ONL, and retinal vessels of each experimental group were detected by TEM. Scale bar=2 μm.

whereas high dose RC28-E resulted in a trendy decrease (P=0.067), in comparison to that in the DM group. FGF Trap, but not VEGF Trap, significantly reduced the free FGF2 protein content in the diabetic retinal homogenate (P<0.05, FGF Trap *vs* DM; P=0.161, VEGF Trap *vs* DM; Figure 5B). These results suggest that RC28-E at all dosages can reduce the concentrations of its free target proteins, *i.e.* VEGF and FGF2, to the normal levels in early diabetic retinas; whereas the single target drugs can only act on their corresponding targets.

Expression of Proinflammatory Factors in the Retinas The expression of the proinflammatory factor intercellular cell adhesion molecule-1 (ICAM-1) and tumor necrosis factor-α (TNF-α) exhibited a similar trend. Both were dramatically upregulated in early diabetic retinas (Both P<0.05, normal *vs* DM; Figure 6A and 6B), which was then substantially decreased by RC28-E at all dosages (All P<0.05, RC28-E at all dosages *vs* DM; Figure 6A and 6B). VEGF Trap and FGF Trap also inhibited the upregulated expression of both proinflammatory factors, however to a less extent than RC28-E

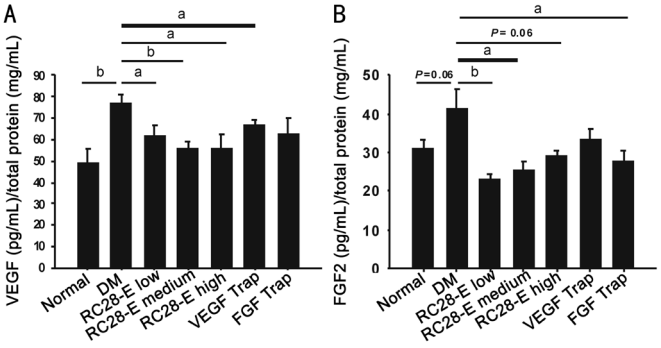

Figure 5 VEGF and FGF2 protein levels in the retinas of each experimental group The protein contents of free VEGF (A) and FGF2 (B) were measured by ELISA kits, normalized by total protein concentration. $^{a}P<0.05$, $^{b}P<0.01$.

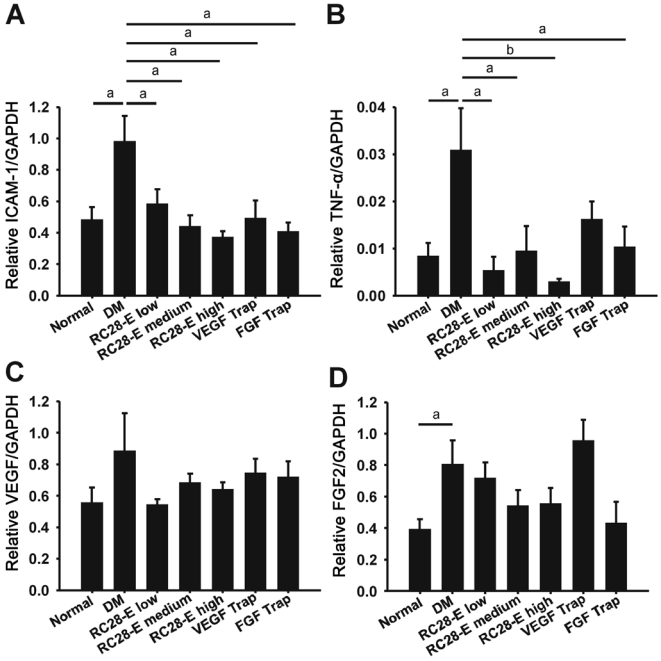

Figure 6 The expression of proinflammatory factors in the retinas of experimental groups The transcript levels of ICAM-1(A), TNF-α (B), VEGF (C), and FGF2 (D) in each experimental group were examined by qPCR, normalized to that of GAPDH. $^{a}P<0.05$, $^{b}P<0.01$.

did (Figure 6A and 6B). Moreover, no significant difference was found in VEGF transcript levels among the experimental groups, except a trendy increase in the DM group (Figure 6C), this result was consistent with our recent study and presumably due to the selection of VEGF reference sequence for qPCR primer design[24]. In contrast, FGF2 mRNA abundance was significantly augmented in the DM group ($P<0.05$, normal *vs* DM; Figure 6D), which was tapered by RC28-E in a dose-dependent manner, although there was no statistical significance among the experimental groups. FGF Trap intervention lowered the FGF2 transcript level, whereas VEGF Trap did not, in early diabetic retinas (Figure 6D).

DISCUSSION

The Fab fragment of RC28-E contains extracellular domain 2 of VEGFR1 and extracellular domain 3 of VEGFR2, the structure that is identical to that in VEGF Trap. In addition, the RC28-E Fab incorporates extracellular domains 2 and 3 of FGFR1. The Fab of RC28-E is fused to the Fc portion of human IgG1. Therefore, RC28-E can bind both VEGF and FGF2 with high affinity without eliciting the downstream signaling pathways of either factor[21]. In the current study, we administered the innovative drug RC28-E to STZ-induced diabetic rats, and reported the remarkable protection of early diabetic retina from apoptotic cell death in vascular network, aberrant activation of glial cell, BRB breakdown and vessel leakage, impairment in the ultrastructures of microvessels and neuroretina, and exacerbation of proinflammatory microenvironment.

Intravenous injection of STZ into the SD rats triggered selective death of islet β cells in pancreas, causing hyperglycemia due to the absolute deficiency of insulin secretion (Table 3). The rats also exhibited weight loss (Table 2), polydipsia (Table 4), polyuria, hyperphagia, and other typical metabolic symptoms of DM[27]. The STZ-induced type 1 diabetic rat model does not experience self-remission or recovery over time as a result of the STZ-induced permanent destruction of islet β cells. Intravitreal injections of RC28-E, VEGF Trap, and FGF Trap had no significant effect on systemic symptoms and metabolic parameters in diabetic rats (Tables 2-4), indicating that these decoy receptors to VEGF, FGF2, or both exert their effects through local, instead of systemic, mechanisms.

At the tissue level in the retina of early diabetic rats, intravitreal injections RC28-E at medium and high doses significantly decreased the number of apoptotic cells in the vasculature (Figure 1), and the protective effects were similar to FGF Trap and better than VEGF Trap (Figure 1). On the other hand, the GFAP staining intensity, an indicator of glial cell reactive activation[28], was substantially subdued by RC28-E at all doses and VEGF Trap; whereas FGF Trap exerted an apparently less inhibition on reactive gliosis under early diabetic condition (Figure 2). These results suggest that single target Traps behave differentially on pathological phenotypes in early diabetic retina, and dual blockade with RC28-E at sufficient concentration may generate the optimal effects. Indeed, the transmission electron microscopy (TEM) results revealed dose-dependent changes in the ultrastructures of outer and inner BRB, as well as that of outer neuroretina, with RC28-E at high dose providing the best protection (Figure 4).

However, the results of Evans blue assay were unexpected. Although the dye leakage in retina was boosted 1.5 fold under early diabetic condition, all the drug treatments, except that of RC28-E at high dose, did not alleviate the diabetes-induced retinal vessel leakage (Figure 3). This could be due to the inappropriate timing for intravitreal injections, in view of a recent parallel study testing the anti-leakage function of a naturally-occurring ocular peptide, α-melanocyte-

stimulating hormone in the same diabetic model[24]; or it could be the insufficient concentrations of the single target Traps to counteract the BRB breakdown and vascular leakage in our rat model of diabetes. At the molecular level, RC28-E, with the high affinity and specificity to both VEGF and FGF2, did significantly reduce the free VEGF and FGF2 protein levels in the early diabetic retinas (Figure 5), and the levels of both proteins in the groups treated with RC28-E at all doses were similar to those in the normal controls (Figure 5). Whereas VEGF Trap and FGF Trap only normalized the protein levels of their corresponding target (Figure 5), implicating the specificity of the blockade. Further, it has been shown that during the stage of nonproliferative DR, to which most of the pathological phenotypes in the STZ-induced diabetic rats belong, VEGF can activate the expression of proinflammatory genes, including ICAM-1 and TNF-α through activation of interleukin 1β and nuclear factor-κB[6]. Therefore, blockade of VEGF signaling with either EC28-E at all doses or VEGF Trap leads to significant downregulation of the proinflammatory gene expression (Figure 6). Moreover, FGF2 is able to synergize with VEGF-mediated signaling pathways[29-30], thus sequestering FGF2 with FGF Trap may interfere with VEGF signaling indirectly, thereby also resulting in the downregulation of proinflammatory genes such as ICAM-1 and TNF-α (Figure 6).

One limitation of this study is that it is a short term study, and some protective effects, such as the anti-vascular leakage, have not been optimized. Since DM is a chronic disease, it would be necessary in the future study to optimize the dosage and delivery frequency of the novel drug, and examine the relatively long-term protective effects of RC28-E in the diabetic models. Another limitation is that the molecular and cellular mechanism underlying the RC28-E's protective effects remains unclear. It would be interesting to select one of the cell types protected by RC28-E, for instance, retinal microvessel endothelial cells, and identify the signaling pathway mediating the protective effects of this novel drug in these cells.

In conclusion, RC28-E, a novel recombinant decoy receptor drug blocking the activities of both VEGF and FGF2, reduces apoptotic cell death in retinal vasculature, inhibits reactive gliosis, ameliorates BRB breakdown and vessel leakage, and improves vascular and neuroretina ultrastructures as well as proinflammatory microenvironment in early diabetic retina. These results support further development of RC28-E into a novel and effective drug to DR.

ACKNOWLEDGEMENTS

Authors' contributions: Zhang Y, Jiang J, Li XR, and Fang JM conceived and designed the research. Li XR and Fang JM supervised the research. Yang QH, Zhang Y, Jiang J and Wu MM preformed the experiments. Han Q, Bo QY, Yu GW, Ru YS, Liu X, Huang M and Wang L preformed the experiments and collected the data. Huang M and Wang L coordinated the research. Zhang Y, Jang J and Zhang XM analyzed the data. Yang QH and Wu MM wrote the first draft of the manuscript. Zhang Y extensively revised and formatted versions of the manuscript.

Conflicts of Interest: Yang QH, None; **Zhang Y,** None; **Jiang J,** None; **Wu MM,** None; **Han Q,** None; **Bo QY,** None; **Yu GW,** None; **Ru YS,** None; **Liu X,** None; **Huang M,** None; **Wang L,** None; **Zhang XM,** None; **Fang JM,** None; **Li XR,** None.

REFERENCES

1 Gedebjerg A, Almdal TP, Berencsi K, Rungby J, Nielsen JS, Witte DR, Friborg S, Brandslund I, Vaag A, Beck-Nielsen H, Sorensen HT, Thomsen RW. Prevalence of micro- and macrovascular diabetes complications at time of type 2 diabetes diagnosis and associated clinical characteristics: a cross-sectional baseline study of 6958 patients in the Danish DD2 cohort. *J Diabetes Complications* 2018;32(1):34-40.

2 Hendrick AM, Gibson MV, Kulshreshtha A. Diabetic retinopathy. *Prim Care* 2015;42(3):451-464.

3 Li X, Zarbin MA, Bhagat N. Anti-vascular endothelial growth factor injections: the new standard of care in proliferative diabetic retinopathy? *Dev Ophthalmol* 2017;60:131-142.

4 Ciulla TA, Harris A, McIntyre N, Jonescu-Cuypers C. Treatment of diabetic macular edema with sustained-release glucocorticoids: Intravitreal triamcinolone acetonide, dexamethasone implant, and fluocinolone acetonide implant. *Expert Opin Pharmacother* 2014;15(7):953-959.

5 Stewart MW. Corticosteroid use for diabetic macular edema: old fad or new trend? *Curr Diab Rep* 2012;12(4):364-375.

6 Tan GS, Cheung N, Simo R, Cheung GC, Wong TY. Diabetic macular oedema. *Lancet Diabetes Endocrinol* 2017;5(2):143-155.

7 Antonetti DA, Klein R, Gardner TW. Diabetic retinopathy. *N Engl J Med* 2012;366(13):1227-1239.

8 Xu Y, Cheng Q, Yang B, Yu S, Xu F, Lu L, Liang X. Increased sCD200 levels in vitreous of patients with proliferative diabetic retinopathy and its correlation with VEGF and proinflammatory cytokines. *Invest Ophthalmol Vis Sci* 2015;56(11):6565-6572.

9 Bressler SB, Liu D, Glassman AR, Blodi BA, Castellarin AA, Jampol LM, Kaufman PL, Melia M, Singh H, Wells JA. Change in diabetic retinopathy through 2 years: secondary analysis of a randomized clinical trial comparing aflibercept, bevacizumab, and ranibizumab. *JAMA Ophthalmol* 2017;135(6):558-568.

10 Li X, Xu G, Wang Y, Xu X, Liu X, Tang S, Zhang F, Zhang J, Tang L, Wu Q, Luo D, Ke X. Safety and efficacy of conbercept in neovascular age-related macular degeneration: results from a 12-month randomized phase 2 study: AURORA study. *Ophthalmology* 2014;121(9):1740-1747.

11 Das A, McGuire PG, Rangasamy S. Diabetic macular edema: pathophysiology and novel therapeutic targets. *Ophthalmology* 2015;122(7):1375-1394.

12 Kirwin SJ, Kanaly ST, Linke NA, Edelman JL. Strain-dependent increases in retinal inflammatory proteins and photoreceptor FGF-2 expression in streptozotocin-induced diabetic rats. *Invest Ophthalmol Vis Sci* 2009;50(11):5396-5404.

13 Lowe WJ, Florkiewicz RZ, Yorek MA, Spanheimer RG, Albrecht BN. Regulation of growth factor mRNA levels in the eyes of diabetic rats. *Metabolism* 1995;44(8):1038.

14 Wohlfart P, Lin J, Dietrich N, Kannt A, Elvert R, Herling AW, Hammes HP. Expression patterning reveals retinal inflammation as a minor factor in experimental retinopathy of ZDF rats. *Acta Diabetol* 2014;51(4): 553-558.

15 Boulton M, Gregor Z, McLeod D, Charteris D, Jarvis-Evans J, Moriarty P, Khaliq A, Foreman D, Allamby D, Bardsley B. Intravitreal growth factors in proliferative diabetic retinopathy: correlation with neovascular activity and glycaemic management. *Br J Ophthalmol* 1997;81(3):228-233.

16 Simó R, Carrasco E, García-Ramírez M, Hernández C. Angiogenic and antiangiogenic factors in proliferative diabetic retinopathy. *Curr Diabetes Rev* 2006;2(1):71-98.

17 Schaper W. Angiogenesis in the adult heart. *Basic Res Cardiol* 1991;86 Suppl 2:51-56.

18 Deissler HL, Deissler H, Lang GK, Lang GE. Ranibizumab efficiently blocks migration but not proliferation induced by growth factor combinations including VEGF in retinal endothelial cells. *Graefes Arch Clin Exp Ophthalmol* 2013;251(10):2345-2353.

19 Deissler HL, Deissler H, Lang GK, Lang GE. VEGF but not PlGF disturbs the barrier of retinal endothelial cells. *Exp Eye Res* 2013;115:162-171.

20 Presta M, Andres G, Leali D, Dell'Era P, Ronca R. Inflammatory cells and chemokines sustain FGF2-induced angiogenesis. *Eur Cytokine Netw* 2009;20(2):39-50.

21 Li D, Xie K, Zhang L, Yao X, Li H, Xu Q, Wang X, Jiang J, Fang J. Dual blockade of vascular endothelial growth factor (VEGF) and basic fibroblast growth factor (FGF-2) exhibits potent anti-angiogenic effects. *Cancer Lett* 2016;377(2):164-173.

22 Schicht M, Hesse K, Schröder H, Naschberger E, Lamprecht W, Garreis F, Paulsen FP, Bräuer L. Efficacy of aflibercept (EYLEA®) on inhibition of human VEGF in vitro. *Ann Anat* 2017;211:135-139.

23 Li D, Wei X, Xie K, Chen K, Li J, Fang J. A novel decoy receptor fusion protein for FGF-2 potently inhibits tumour growth. *Br J Cancer* 2014;111(1):68-77.

24 Cai S, Yang Q, Hou M, Han Q, Zhang H, Wang J, Qi C, Bo Q, Ru Y, Yang W, Gu Z, Wei R, Cao Y, Li X, Zhang Y. Alpha-melanocyte-stimulating hormone protects early diabetic retina from blood-retinal barrier breakdown and vascular leakage via MC4R. *Cell Physiol Biochem* 2018;45(2):505-522.

25 Zhang L, Dong L, Liu X, Jiang Y, Zhang L, Zhang X, Li X, Zhang Y. Alpha-Melanocyte-stimulating hormone protects retinal vascular endothelial cells from oxidative stress and apoptosis in a rat model of diabetes. *PLoS One* 2014;9(4):e93433.

26 Xu L, Zhang Y, Guo R, Shen W, Qi Y, Wang Q, Guo Z, Qi C, Yin H, Wang J. HES1 promotes extracellular matrix protein expression and inhibits proliferation and migration in human trabecular meshwork cells under oxidative stress. *Oncotarget* 2017;8(13):21818-21833.

27 Yasuda H, Jin Z, Nakayama M, Yamada K, Kishi M, Okumachi Y, Arai T, Moriyama H, Yokono K, Nagata M. NO-mediated cytotoxicity contributes to multiple low-dose streptozotocin-induced diabetes but not to NOD diabetes. *Diabetes Res Clin Pract* 2009;83(2):200-207.

28 Lahmar I, Pfaff AW, Marcellin L, Sauer A, Moussa A, Babba H, Candolfi E. Muller cell activation and photoreceptor depletion in a mice model of congenital ocular toxoplasmosis. *Exp Parasitol* 2014;144:22-26.

29 Holmes DI, Zachary IC. Vascular endothelial growth factor regulates stanniocalcin-1 expression via neuropilin-1-dependent regulation of KDR and synergism with fibroblast growth factor-2. *Cell Signal* 2008;20(3):569-579.

30 Kano MR, Morishita Y, Iwata C, Iwasaka S, Watabe T, Ouchi Y, Miyazono K, Miyazawa K. VEGF-A and FGF-2 synergistically promote neoangiogenesis through enhancement of endogenous PDGF-B-PDGFRbeta signaling. *J Cell Sci* 2005;118(Pt 16):3759-3768.